Geophysical Research Letters

RESEARCH LETTER
10.1029/2023GL103470

High-Resolution Broadband Lg Attenuation Structure of the Anatolian Crust and Its Implications for Mantle Upwelling and Plateau Uplift

Wei-Mou Zhu[1,2], Lian-Feng Zhao[1,3], Xiao-Bi Xie[4], Xi He[1], Lei Zhang[1,5], and Zhen-Xing Yao[1]

[1]Key Laboratory of Earth and Planetary Physics, Institute of Geology and Geophysics, Chinese Academy of Sciences, Beijing, China, [2]College of Earth and Planetary Sciences, University of Chinese Academy of Sciences, Beijing, China, [3]Heilongjiang Mohe Observatory of Geophysics, Institute of Geology and Geophysics, Chinese Academy of Sciences, Beijing, China, [4]Institute of Geophysics and Planetary Physics, University of California at Santa Cruz, Santa Cruz, CA, USA, [5]School of Earth and Space Sciences, Institute of Theoretical and Applied Geophysics, Peking University, Beijing, China

Abstract The Anatolian Plateau, currently experiencing rapid uplift and westward escape, records both the termination of oceanic subduction and the conversion to continental collision. The crustal response to the transition of the subduction environment from eastern to western Anatolia can be inferred by the seismic velocity and attenuation structures. With this study, we construct a broadband Lg-wave attenuation model for the Anatolian Plateau and use it to constrain lateral crust heterogeneities linked to this transition. Crustal Lg attenuation links late Cenozoic magmatism with asthenospheric upwelling by characterizing the lithospheric thermal structure. The widely distributed strong attenuation observed in eastern Anatolia may be related to the crustal partial melting due to mantle upwelling after the delamination and subsequent break-off of the Bitlis slab. Lithospheric dripping in central Anatolia likely facilitates the mantle flows through the window between the Cyprus and Aegean slabs, which results in the piecemeal low Q_{Lg} anomaly in central Anatolia.

Plain Language Summary Different parts of the Anatolian Plateau are in different evolution stages between oceanic subduction and continental collision and currently undergoing plateau uplift and tectonic escape. The regional seismic velocity and attenuation can be used to characterize crustal partial melting and lateral heterogeneity, which can further identify the underlying subduction process. In this study, we construct a high-resolution broadband Lg-wave attenuation model for the Anatolian Plateau. Strong Lg attenuation in Anatolia correlates well with late Cenozoic magmatism distributions and can be an indicator of high temperature or partial melting in the crust. Combined with previous studies, we suggest that the mantle upwelling induced by the delamination of the Bitlis slab is likely reworking the crust in eastern Anatolia and is the cause of widespread thermal anomalies there. The lithospheric dripping process in central Anatolia may facilitate the mantle flows through the window between the Cyprus and Aegean slabs, and results in a piecemeal low Q_{Lg} anomaly pattern in central Anatolia.

Key Points:

- A high-resolution broadband Lg-wave attenuation model is constructed for the Anatolian Plateau
- Widespread strong attenuation in the eastern Anatolian crust is likely related to slab delamination
- The circular-shaped attenuation anomaly may result from slab tearing and lithospheric dripping beneath central Anatolia

Supporting Information:

Supporting Information may be found in the online version of this article.

Correspondence to:

L.-F. Zhao,
zhaolf@mail.iggcas.ac.cn

Citation:

Zhu, W.-M., Zhao, L.-F., Xie, X.-B., He, X., Zhang, L., & Yao, Z.-X. (2023). High-resolution broadband Lg attenuation structure of the Anatolian crust and its implications for mantle upwelling and plateau uplift. *Geophysical Research Letters*, *50*, e2023GL103470. https://doi.org/10.1029/2023GL103470

Received 26 FEB 2023
Accepted 10 MAR 2023

Author Contributions:

Conceptualization: Wei-Mou Zhu, Lian-Feng Zhao, Xiao-Bi Xie
Data curation: Wei-Mou Zhu, Lei Zhang
Formal analysis: Wei-Mou Zhu, Xi He, Lei Zhang
Funding acquisition: Lian-Feng Zhao, Zhen-Xing Yao
Investigation: Wei-Mou Zhu
Methodology: Wei-Mou Zhu, Lian-Feng Zhao, Xiao-Bi Xie, Lei Zhang
Project Administration: Lian-Feng Zhao, Zhen-Xing Yao
Resources: Wei-Mou Zhu, Lian-Feng Zhao
Software: Wei-Mou Zhu, Lian-Feng Zhao, Xi He, Lei Zhang

1. Introduction

Located in the central part of the Alpine-Himalayan orogenic belt, the Anatolian plate is typically on the terminal stage of the Wilson cycle, which marks the onset of continental collision as oceanic subduction terminates (Burke, 2011). Multiple plate-mantle interactions, for example, slab roll-back, tear and break-off, lithospheric delamination, and local convective instabilities, can be triggered by a significant change in subduction environment, such as the transition from oceanic to continental subductions (van Hunen & Miller, 2015). These geodynamic processes control the evolution of the entire Anatolian Plateau. Typically, slab tears can be interpreted beneath southwestern Anatolia down to depths 150–180 km from various tomography models and deep earthquake activities (Bocchini et al., 2018; Hayes et al., 2018; Kounoudis et al., 2020). Driven by the Arabia-Eurasia collision in the east and oceanic subduction along the Hellenic Trench and Cyprus Arc in the southwest, the Anatolian Plateau is undergoing tectonic escape, including westward translation and counterclockwise rotation (Reilinger et al., 2006). Receiver function and other studies across the Anatolian plateau have suggested that there is no rapid change in the crust thickness within eastern and central Anatolia (Figure S1 in Supporting Information S1, e.g., Laske et al., 2013; Vanacore et al., 2013). The east Anatolian fault zone and north Anatolian fault zone accommodate the tectonic escape and divide the Anatolian plate into four distinct Neotectonic provinces,

Supervision: Lian-Feng Zhao, Xiao-Bi Xie, Zhen-Xing Yao
Validation: Wei-Mou Zhu
Visualization: Wei-Mou Zhu
Writing – original draft: Wei-Mou Zhu, Xi He, Lei Zhang
Writing – review & editing: Wei-Mou Zhu, Lian-Feng Zhao, Xiao-Bi Xie, Xi He, Lei Zhang

including the East, North, Central, and West Anatolian Provinces (EAP, NAP, CAP, and WAP), respectively (Bozkurt, 2001). The widespread late Cenozoic magmatism migrated from east to west Anatolia, forming the eastern Anatolian volcanic province, Cappadocia volcanic province, and Galatian volcanic province in central Anatolia (Figure 1, inset). This magmatism indicates the westward progression of oceanic slab rupture and the upwelling of hot asthenospheric mantle material (Rabayrol et al., 2019). However, due to the complex mutual relationship between the evolution of the slab and the deformation of the overriding plate, it remains unclear regarding the details of plateau uplift and related magmatism rise (Schildgen et al., 2014). To solve these puzzles, more constraints from geophysical observations are required.

The unique landform and magmatism distributions in Anatolia are regarded as the consequence of the subduction and lithospheric foundering process, which often change the thermal status and rheological properties of the crust (Delph et al., 2017; Fernández-Blanco et al., 2020; Göğüş et al., 2017). A single delamination event has been proposed to account for the uplift of both central and eastern Anatolia (Bartol & Govers, 2014). The inflow of the hot asthenospheric material in this model can provide the required buoyancy and heat for the uplift. However, Göğüş et al. (2017) argued that the break-off process is generally constrained in the plate convergence zone and suggested that the development of the lithospheric instability as a diversity of "drip tectonics" to account for the Central Anatolia Plateau (CAP) uplift and massive volcanisms along the plateau margins since ∼10 Ma. Geodynamic processes, for example, the lithospheric dripping, slab roll-back, and break-off, are often accompanied by exchanges of heat and materials, partial melting in the crust and upper mantle, and diversified magmatic expressions (van Hunen & Miller, 2015; Wang & Currie, 2015). Therefore, identifying existing crustal thermal anomalies or partial melting can help distinguish the geodynamic processes beneath central and eastern Anatolia (Kounoudis et al., 2020).

Seismic attenuation is very sensitive to high-temperature anomalies and partial melting in the crust and upper mantle (e.g., Artemieva et al., 2004; He et al., 2021; Takei, 2017). Studies on regional seismic attenuation using the Pn, Pg, Sn, and Lg phases have been conducted in Anatolia and the entire Middle East (e.g., Al-Damegh et al., 2004; Bao et al., 2011; Gök et al., 2003; Zor et al., 2007). As the most prominent seismic phase on regional seismograms, the Lg-wave can be considered as multiply reflected S-waves trapped in the crust waveguide (e.g., Bouchon, 1982; Zhang & Lay, 1995). Therefore, the Lg-wave can provide a unique measurement on the attenuation in the crust and thus has been widely used in crustal attenuation studies (Bao et al., 2012; Baumont et al., 1999; Chen et al., 2021; He et al., 2021; Zhao & Xie, 2016). However, due to the sparse data coverage, existing Lg attenuation results around Anatolia were mostly in low resolution (Kaviani et al., 2015; Pasyanos et al., 2009; Zor et al., 2007). To investigate the geodynamic problem and accompanied thermal structures related to the plateau uplift, plate extrusion, and magmatism in Anatolia, high-resolution crust attenuation imaging is highly demanded. In this study, benefitted from the high-density seismic network and accumulated broadband data, we combine both single-station and two-station Lg-wave spectral data to develop a high-resolution broadband (0.05–10.0 Hz) Lg attenuation tomography image for the Anatolian region. Along with regional tectonic deformation, seismicity, and other geophysical and geology observations, we explore crustal attenuation structures and their implications to the geodynamics in the Anatolian region.

2. Data and Methods

Thank the International Federation of Digital Seismograph Networks (FDSN) webservices and the Mass Downloader module of Obspy (Krischer et al., 2015), we can now readily collect most of the available regional waveform data from a variety of networks and data centers. The data set consists of 56,341 seismograms recorded at 650 stations from 521 regional crustal earthquakes between January 2000 and December 2020. The Moho depth data are from the Crust1.0 model. Figure S2 in Supporting Information S1 shows the distribution of seismic stations and their affiliated networks and earthquakes used in this study. The information on seismic stations, their affiliated networks, earthquakes, and data resources are listed in Tables S1, S2, and S3, respectively in Supporting Information S1. To improve the signal-to-noise ratio (SNR) and avoid the influence of complex rupture processes of large earthquakes, only earthquakes with magnitudes between m_b 4.0 and 6.5 were used.

We used a 3.0–3.6 km/s group velocity window to sample the Lg-wave signal. An equal-length time window was also used to extract the pre-Pn and pre-Lg noises, respectively (Figure S3 in Supporting Information S1). Then, we calculated Fourier spectra for Lg-waves and noise series, and the Lg spectra were corrected for the noise effects (Text S1 and Figure S4 in Supporting Information S1). A two-step inversion method was adopted. First,

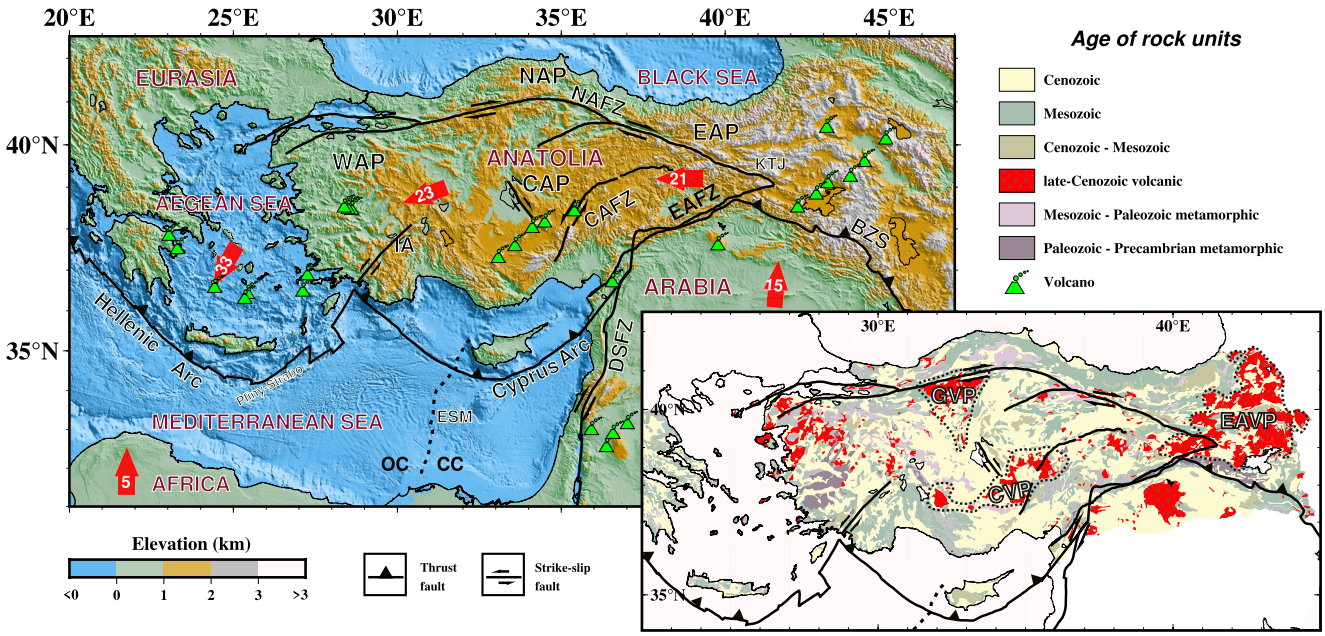

Figure 1. Map showing the topography and major tectonic and geological features in the Anatolian Plateau and surrounding regions. The green volcano symbols show volcano locations and red arrows with numbers represent plate movement velocities (mm/yr) with respect to a stable Eurasian plate (Reilinger et al., 2006). The black dashed line denotes the transition from OC (oceanic crust) to CC (continental crust) (Granot, 2016). BZS: Bitlis-Zagros suture; EAFZ: East Anatolian fault zone; NAFZ: North Anatolian fault zone; CAFZ: Central Anatolian fault zone; ESM: Eratosthenes Seamount; IA: Isparta Angle; KTJ: Karliova Triple Junction. The inset map illustrates simplified geological units in the Anatolian region (Pawlewicz et al., 1997). CVP: Cappadocia Volcanic Province; GVP: Galatian Volcanic Province.

joint inversions were performed to the observed Lg wave spectra to obtain the Lg-wave Q and source term (Zhao, Xie, Wang, et al., 2013). Next, at each frequency, the Least Squares QR factorization algorithm (LSQR) with regularization, damping, and smoothing was used to solve the linear inversion system (Figure S5 in Supporting Information S1, e.g., Paige & Saunders, 1982), which converts the path Lg Q into a Q distribution map. After the inversion, the data residuals were largely reduced and tend to be a zero-mean Gaussian function with a smaller standard deviation (Figure S6 in Supporting Information S1). This inversion was independently repeated for individual frequencies to obtain a broadband Q model. The similar Lg-wave tomography method has been successfully applied in Northeast China (Zhao et al., 2010), North China (Zhao, Xie, Wang, et al., 2013), the Tibetan Plateau (He et al., 2021; Zhao, Xie, He, et al., 2013), Mongolia (L. Zhang et al., 2022), Southeast Asia (Luo et al., 2021), the Middle East (Zhao & Xie, 2016), the Australian continent (Wei et al., 2017) and eastern North America (Zhao & Mousavi, 2018).

A checkerboard method was used to examine the resolution of the Lg-wave attenuation model at individual frequencies (e.g., Zhao et al., 2010). A theoretical model can be constructed by adding ±7% checkerboard-shaped logarithmic attenuation perturbations to a background Q, from which we obtained a synthetic data set (e.g., He et al., 2021). Then, 5% root mean square random noise was added to the synthetic amplitude to simulate the real data. Finally, this synthetic data set was used as the input of the tomographic system, and the inversion result was compared to the original checkerboard model to estimate the resolution (Figure 2e). The resolution is dependent on ray coverage and is frequency dependent, but usually can reach 1.0° × 1.0° in the study area (Figure S7 in Supporting Information S1).

3. Results

A high-resolution broadband Lg-wave attenuation model composed of 58 individual frequencies between 0.05 and 10.0 Hz is obtained for the Anatolian Plateau and its surrounding regions. The Lg signal is usually dominated between frequencies 0.2 and 2.0 Hz, within which the obtained attenuation model is most robust (Figure S8 in Supporting Information S1). The Q_{Lg} images at individual frequencies show strong lateral variations, with distinct features in different geo-blocks, and correlate well with regional tectonics (Figures 2a–2c). We compared their frequency dependencies for eight main geo-blocks (Figure S9a in Supporting Information S1). The Q_{Lg} values

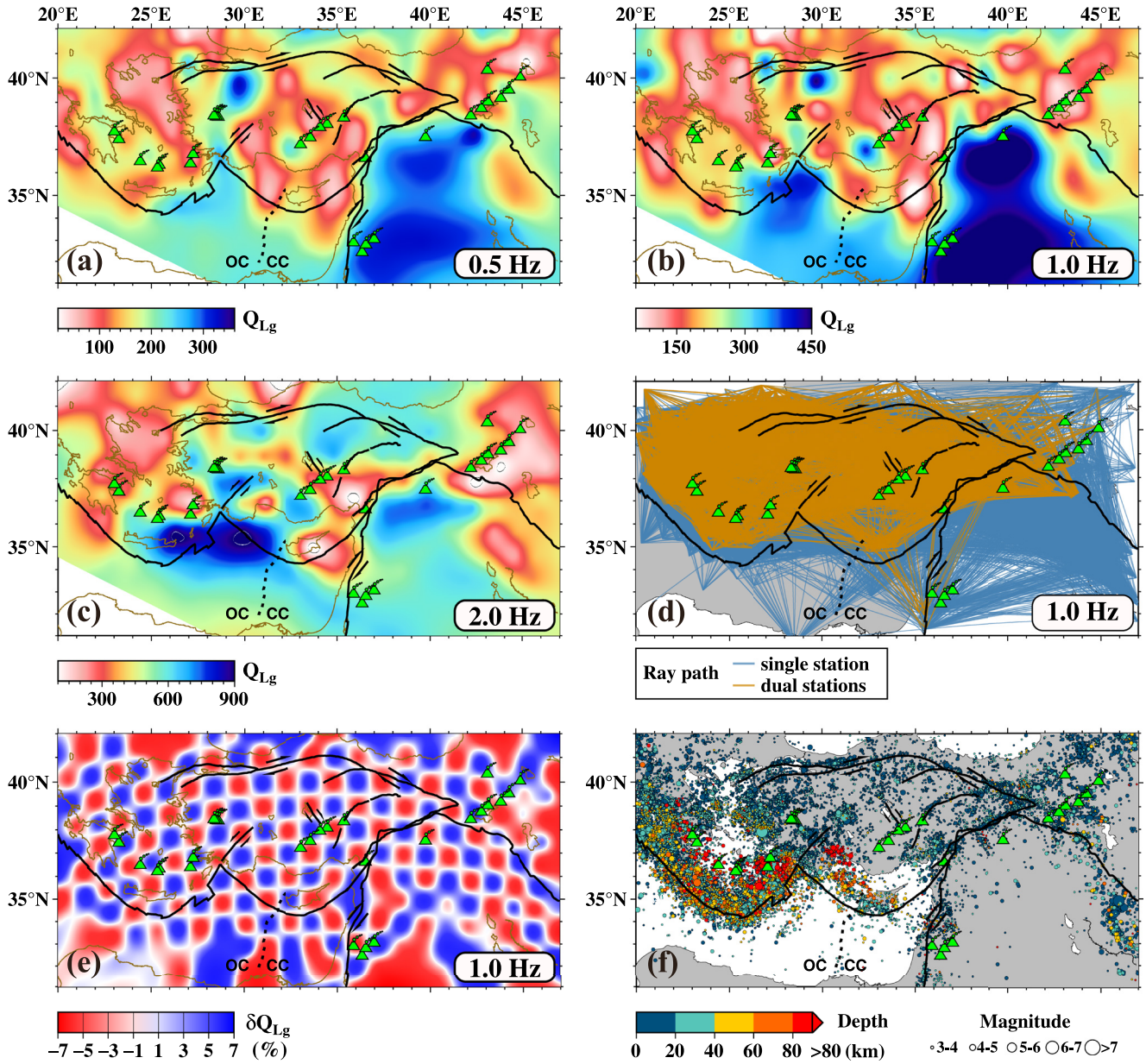

Figure 2. Lateral variations of Q_{Lg} in the Anatolian Plateau and surrounding regions at 0.5 Hz (a), 1.0 Hz (b), and 2.0 Hz (c). Note that different color scales are used for each Q_{Lg} map. (d) Ray path density at 1.0 Hz, where single- and two-station data are represented by blue and yellow lines. (e) 1.0° × 1.0° checkerboard resolution test at 1.0 Hz. (f) Seismicity over the past two decades around Anatolia. Hypocenters and magnitudes are obtained from the International Seismological Centre (ISC) catalog.

generally increase with the increasing frequency and characterize the geo-blocks better within the 0.2–2.0 Hz band than those outside this band (Figure S9b in Supporting Information S1). Therefore, the Q_{Lg} in this band is selected (Figure 3) to distinguish different tectonic provinces.

The previous Lg attenuation studies revealed an overall strong attenuation pattern in and around the Anatolian Plateau (Kaviani et al., 2015; Pasyanos et al., 2009; Zhao & Xie, 2016; Zor et al., 2007). Our new broadband Lg-wave attenuation model correlates well with previous results but has a higher resolution of approximately 1.0° × 1.0° (Figure 2e). Therefore, it exhibits more attenuation details and permits us to discuss the related geodynamic processes and tectonic phenomena up to a whole new level.

The most prominent feature in our broadband attenuation model is the great contrast between the Arabian plate and the Anatolian region. The Bitlis-Zagros suture marks the front edge of the colliding Arabian plate, and the

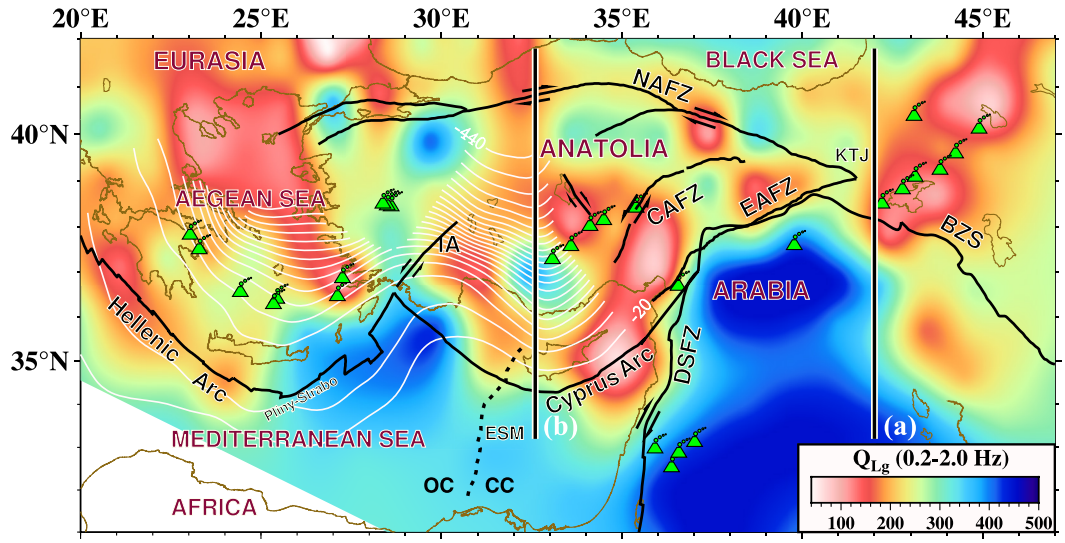

Figure 3. Broadband Q_{Lg} map between 0.2 and 2.0 Hz in the Anatolian Plateau and surrounding regions. Also shown in the map are depth contours of Aegean and Cyprus slabs (white lines) obtained from the Slab2 model (Hayes et al., 2018), and the locations of two longitudinal profiles a and b in Figure 4 (two straight black lines).

Dead Sea fault zone linked with the eastern Anatolian fault zone marks the plate boundary between the Arabian plate and the eastern Mediterranean. The abrupt attenuation boundaries coincide well with these sharp plate boundaries. Overall, the Anatolian Plateau exhibits much stronger Lg-wave attenuation in comparison to the weak attenuation in the Arabian plate, but internally, the attenuation still varies from east to west. Almost the entire eastern Anatolia, separated by the north Anatolian fault zone and east Anatolian fault zone, is characterized by low Q_{Lg}, while central and western Anatolia exhibit unevenly distributed low Q_{Lg} values. Strong attenuation was observed in the Aegean Sea block, where the crust thickness sharply decreases to ~25 km (Figure S1 in Supporting Information S1), which affects Lg propagation and its amplitude decay (Kennett, 1989; Zhang & Lay, 1995). Some researchers reported inefficient Lg wave propagation in the Anatolian Plateau and even Lg-wave blockage for ray paths across the southern Black Sea and the Bitlis-Zagros thrust (Al-Damegh et al., 2004; Zor et al., 2007). However, when relatively larger earthquakes were used, weak Lg signals can still be observed in seismograms passing through a short distance in the relatively thin crust, which is similar to the situation found in Southeast Asia (Luo et al., 2021). Few or no deep (>60 km) earthquakes are observed beneath eastern Anatolia (Figure 2f). The Bitlis slab may have completely broken off and induced extensive mantle upwelling, leading to strong attenuation in the current crust (Figure 3). In contrast, segmented Aegean and Cyprus slabs still exist, which can be reflected by the extensive deep earthquake activity in southeastern Anatolia (Figure 2f, e.g., Bocchini et al., 2018). The piecemeal low Q_{Lg} values in the crust indicate the linkage between deep thermal transport and surface magmatism in the central Anatolian plate.

4. Discussion

4.1. Weak Crust and Intact Lithospheric Delamination in Eastern Anatolia

The combination of the Arabia-Anatolian collision and Bitlis slab delamination, together with subsequent break-off, deformed the landscape of eastern Anatolia (Barazangi et al., 2006; Göğüş & Pysklywec, 2008; Göğüş & Ueda, 2018; Keskin, 2003, 2007; Lei & Zhao, 2007; Memiş et al., 2020; Şengör et al., 2008). As a result, these dynamic processes generated deep mantle upwelling and intrusion into the crust, causing intraplate magmatism and ultimately forming the eastern Anatolian volcanic province (Nikogosian et al., 2018). We observed widespread low Q_{Lg} values across the entire EAP and they correspond well with the low S-wave velocities in the crust, which implies extensive crustal partial melting in this region (Angus et al., 2006; Delph et al., 2015). High conductivity zones obtained based on magnetotelluric data revealed the locally fluid-rich EAP (Hacıoğlu et al., 2018; Türkoğlu et al., 2008). Additionally, low S-wave velocities in the uppermost mantle (Gök et al., 2007), low Pn-wave velocities (Lü et al., 2017; Mutlu & Karabulut, 2011), and strong Sn attenuation (Al-Damegh

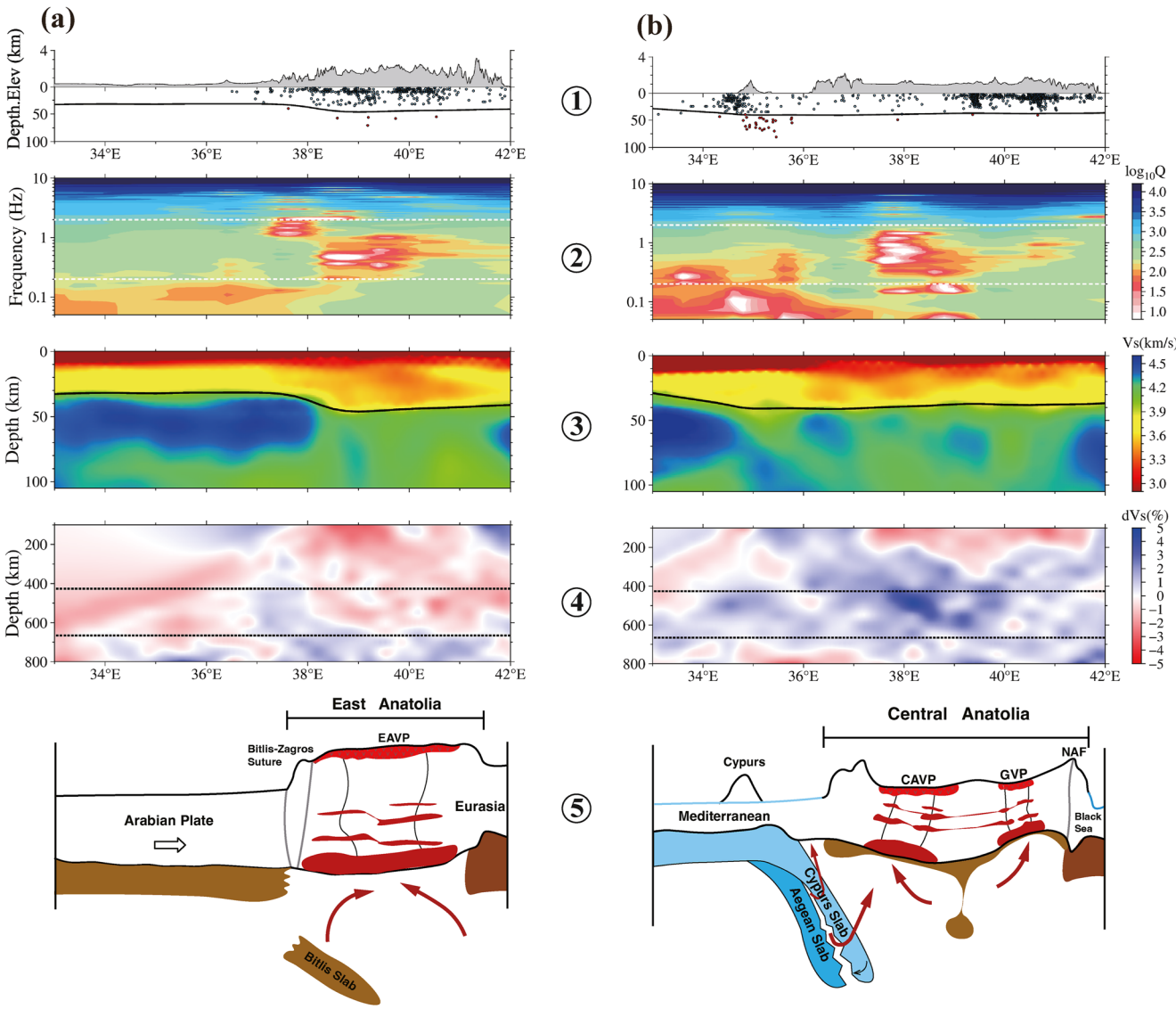

Figure 4. Comparisons of two longitudinal cross sections in (a) the east and (b) central Anatolian region, with their locations are marked in Figure 3. From top to bottom are ① topography and seismicity, ② Q_{Lg} versus frequency, ③ lithospheric S-wave velocity (Kaviani et al., 2020), ④ mantle S-wave velocity perturbation (Kounoudis et al., 2020), and ⑤ sketches showing dynamic models for the collision/subduction shifted from east to central Anatolia.

et al., 2004; Gök et al., 2003; Kaviani et al., 2022) reflect an anomalously hot and partially molten uppermost mantle in the EAP. Upwelling of the sublithospheric mantle may have significantly reworked the EAP, causing thermal weakening and partial melting in the crust, thus strongly attenuating the wave propagation. According to the low S-wave velocity in the lower crust of the EAP, the melt percentage is roughly between 5% and 8% (Delph et al., 2015), which is close to the melt percentage of 3%–10% from low-resistivity observations (Türkoğlu et al., 2008). The degree of crustal melting of ~7% suggests that the crustal strength is significantly reduced (Rosenberg & Handy, 2005), and weak areas may permit the localized flow of crustal materials (Hacıoğlu et al., 2018). Therefore, it is suspected that slab break-off leads to widespread partial melting in the EAP crust, which exhibits substantially low Q_{Lg} values across that region (Figure 4a). Considering these observations, we suggested that a weak and fluid-rich crust allowed for late Cenozoic uplift and magmatism, which were induced by slab delamination and subsequent break-off processes in eastern Anatolia (Göğüş & Pysklywec, 2008; Kaviani et al., 2020; Schleiffarth et al., 2018).

On the southeastern margin of the Tibetan Plateau, strong crustal attenuation revealed low strength and partial melting in the crust, indicating a weak crust, and possible crustal flow (He et al., 2021; Zhao, Xie, He,

et al., 2013). Similarly, Anatolia also experienced continental collision, strong crustal deformation, and westward tectonic escape. While the average Q_{Lg} increases generally from the EAP to the CAP, then to the WAP (Figure S10 in Supporting Information S1), their detailed distributions are different. The widespread low Q_{Lg} values in the EAP transferred to patchy and discontinuous Q_{Lg} distribution in the CAP. Different attenuation values and patterns may correspond to their changing rheological properties, that is, the strongest Arabia, the relatively weaker CAP and WAP, and the weakest EAP. This may indicate the feasibility of the tectonic escape of CAP and WAP from the EAP (Figure 3). In addition to the northward push from the strong Arabian plate which exhibits extremely weak attenuation, the slab rollback and the underlying mantle return flow also apply forces to the relatively weaker CAP and WAP (Faccenna et al., 2013; Le Pichon & Kreemer, 2010). Since the CAP and WAP are westwards escaping from the fluid-rich and weaker EAP, which is accommodated by the east Anatolian fault zone and north Anatolian fault zone, it's rather difficult for the push force from Arabian plate to make it. However, it's more likely the pull force facilitated the CAP and WAP escaping from EAP. In summary, the westward pull from slab rollback and mantle flow may play a more significant role than the northward push in the kinematic movement of the Anatolian plate.

4.2. Circular Patterned Attenuation Anomaly Linking to the Slab Tearing and Lithospheric Dripping in Central Anatolia

The tectonic environment rapidly changes from oceanic subduction in central Anatolia to post-collision in eastern Anatolia (Şengör et al., 2008). The segmented African oceanic lithosphere was subducted into the asthenosphere at different depths and caused various deformations in the overlying Anatolian lithosphere (Berk Biryol et al., 2011). High-velocity anomalies from the tomography revealed that the African oceanic lithosphere subducted beneath the eastern Mediterranean, whereas the Aegean and Cyprus slabs are separated by a slab window and ongoing subduction. The Bitlis slab is more fragmented and is strongly deformed beneath the northeastern Cyprus Arc (Hayes et al., 2018; Portner et al., 2018). Geochemical analysis showed that the westward migrated Cenozoic magmatism is concomitant with slab tears and break-offs (Rabayrol et al., 2019). The slab tearing and lithosphere evolution is tightly linked to the uplift and interior magmatism in the CAP (Figure 4, e.g., Schildgen et al., 2014).

A circular-shaped low Q_{Lg} pattern can be observed around a relatively high Q_{Lg} anomaly centered at 37.0°N 33.5°E in the CAP (Figure 3). This is likely the response to the slab tearing and lithospheric foundering in this region. It is different from eastern Anatolia and has been suggested by previous studies from different aspects, for example, volcano geochemistry (Şen et al., 2004), the high-temperature mantle (Reid et al., 2017), and melt equilibration depths (Reid et al., 2019). Both the lithospheric foundering and volcanism at the CAP margins can be explained by convective removal or Rayleigh-Taylor/gravitational instability (Göğüş et al., 2017). Geodynamic simulations also indicated that gravitational lithosphere removal may lead to a symmetric magmatic expression at the surface, a significantly thinned lithosphere, and a melting crust (Wang & Currie, 2015). It can be accepted that the lithospheric dripping process can result in uneven crustal melting and a unique distribution of late Cenozoic magmatism in the CAP (Göğüş et al., 2017).

The totally broken Bitlis slab and the slab tear or window between Cyprus and the Aegean have been imaged beneath the CAP (Hayes et al., 2018). This window may provide a route for subduction-related hydration and asthenospheric upwelling that weakens the overriding CAP lithosphere and effectively promotes lithospheric instability and subsequent dripping (Kounoudis et al., 2020). From the lithosphere to the asthenosphere, the lithospheric replacement with hot sublithospheric mantle beneath the CAP (Figure 4b③ and ④) can be reflected by both the slow shear wave velocity anomalies around the "V"-shaped fast velocity body (Fichtner et al., 2013; Kaviani et al., 2020) and the negative S-wave velocity perturbations (Kounoudis et al., 2020). Lateral variations in Q_{Lg} anomalies suggest high temperatures and/or partial melting within the crust, which can be strongly affected by the dripping and slab tearing process (Figures 3 and 4b). Low Q_{Lg} zones in the CAP correspond well to Neogene-Quaternary volcanisms, including the Galatian volcanic province and Cappadocia volcanic province, which are localized along the northern and southern margins. These volcanic rocks are coeval and are partially derived from asthenospheric mantle sources (Kürkcüoglu et al., 2004; Toprak et al., 1996; Varol et al., 2014). The slow Vs and high Vp/Vs ratio in the crust and uppermost mantle beneath central Anatolia may indicate partial crustal melt (2%–6%) and uppermost mantle partial melting (<1%), that is, underlying massive magma originating from the asthenosphere for these volcanic rocks (Zhu, 2018). Moreover, sediment accretion in the Cyprus

subduction zone raises the crustal temperature and leads to thermally activated viscous flow in the lower crust, thus causing the high forearc uplift of the southern CAP margin (Fernández-Blanco et al., 2020). This thermal effect on the crust may enhance the observed low Q_{Lg} values there. The circular thermal anomaly and other piecemeal anomalies revealed by strong Lg attenuation are consistent with the fact that the asthenospheric material was facilitated by not only the slab tearing but also the lithospheric mantle viscous dripping, and subsequently upwelled and intruded into the crust.

The Q_{Lg} changes rapidly from the eastern Mediterranean in the west to the Arabian plate in the east (Figure 3). Through the Pliny-Strabo transform faults, Cyprus Arc, and Dead Sea fault zone successively, a high-to-low-to-high Q_{Lg} pattern reflects a significant transition of the crustal property, which is related to the stalled subduction across the Cyprus Arc due to the incipient collision of the Eratosthenes seamount (Aksu et al., 2021; Wdowinski et al., 2006). The crustal transition occurred between the relatively strong oceanic crust and the weak and stretched continental crust in the eastern Mediterranean (Granot, 2016). The Dead Sea fault zone accommodates the sinistral displacement between the Arabian plate and the African plate (Smit et al., 2010), where the attenuation changes from low-Q_{Lg} in the eastern Mediterranean to high-Q_{Lg} in the Arabian plate. This marks a sharp change in the subduction environment and crustal properties. Overall, the high-to-low-to-high Q_{Lg} variation reveals a strong-to-weak-to-strong crustal transition, from the ongoing subducting Mediterranean block to the stretched and thinned Cyprus Arc and then to the relatively strong Arabian continent (Figure 4⑤). This process may have facilitated asthenospheric mantle entrainment under the Anatolian plate, and triggered the initiation of the lithospheric dripping (Göğüş et al., 2017).

5. Conclusions

A broadband Lg attenuation model was obtained in the Anatolian Plateau and its surrounding regions by utilizing a two-step inversion method. The resolution can approach to 1.0° or higher. In line with previous geological and geophysical observations, our crustal Lg attenuation model suggests that low Q_{Lg} regions indicate widespread crustal partial melting in the EAP where the Bitlis slab delaminated and finally broke off. This process contributes to the surface uplift and melts production of the EAP. As the Cyprus slab rollback progresses, hot asthenospheric mantle material flows through the slab window between Cyprus and the Aegean slab, and intrudes and reworks the lithosphere, leading to crustal melting and uplift of the CAP. Crustal melting, revealed by circular-shaped low Q_{Lg} anomalies, is possibly caused by the slab tearing and lithospheric dripping processes in the CAP, which are highly associated with widespread volcanism and the cryptic uplift of the entire CAP. The difference among rheological properties of the EAP, CAP, and WAP revealed by their attenuation structures are likely related to the kinematic movement of the Anatolian plate, that is, the pull from slab rollback and mantle flow dominating the escape of relatively strong CAP and WAP from the weakest EAP rather than the push from the Arabian plate. The high-to-low-to-high pattern of the Lg wave Q along the subducting Mediterranean block, Cyprus Arc and the Arabian plate is consistent with the crust properties in these regions. They contribute to not only plate kinematics but also, more importantly, the geodynamic evolution of the subduction environment transition regions.

Data Availability Statement

Waveform and station metadata were downloaded using the Obspy (Krischer et al., 2015) through the International Federation of Digital Seismograph Networks (FDSN) webservices and obtained from the GEOFON Data Management Center (https://geofon.gfz-potsdam.de/waveform/archive/) and Incorporated Research Institutions for Seismology Data Management Center (IRISDMC; http://www.iris.edu/ds/nodes/dmc/) and the associated networks operators were listed in the Table S3 in Supporting Information S1. The S-wave velocity data (Kaviani et al., 2020) were collected from IRIS Earth Model Collaboration (IRISEMC) data product at http://ds.iris.edu/ds/products/emc-midd_east_crust_1/ (last accessed August 2022). The single- and two-station Lg amplitude data used in this study can be accessed at the World Data Centre for Geophysics, Beijing at https://doi.org/10.12197/2022GA025 (last accessed August 2022). Figures were generated using Generic Mapping Tools (Wessel et al., 2019).

Acknowledgments
The authors thank Editor L. Flesch and two anonymous reviewers for their helpful comments that greatly improved the manuscript. This research was supported by the National Natural Science Foundation of China (41630210, U2139206, 41974061, and 41974054) and the Special Fund of China Seismic Experimental Site (2019CSES0103).

References

Aksu, A. E., Hall, J., & Yaltırak, C. (2021). Miocene–Quaternary tectonic, kinematic and sedimentary evolution of the eastern Mediterranean Sea: A regional synthesis. *Earth-Science Reviews*, *220*, 103719. https://doi.org/10.1016/j.earscirev.2021.103719

Al-Damegh, K., Sandvol, E., Al-Lazki, A., & Barazangi, M. (2004). Regional seismic wave propagation (Lg and Sn) and Pn attenuation in the Arabian Plate and surrounding regions. *Geophysical Journal International*, *157*(2), 775–795. https://doi.org/10.1111/j.1365-246X.2004.02246.x

Angus, D. A., Wilson, D. C., Sandvol, E., & Ni, J. F. (2006). Lithospheric structure of the Arabian and Eurasian collision zone in eastern Turkey from *S* -wave receiver functions. *Geophysical Journal International*, *166*(3), 1335–1346. https://doi.org/10.1111/j.1365-246X.2006.03070.x

Artemieva, I. M., Billien, M., Lévêque, J.-J., & Mooney, W. D. (2004). Shear wave velocity, seismic attenuation, and thermal structure of the continental upper mantle. *Geophysical Journal International*, *157*(2), 607–628. https://doi.org/10.1111/j.1365-246X.2004.02195.x

Bao, X., Sandvol, E., Chen, Y. J., Ni, J., Hearn, T., & Shen, Y. (2012). Azimuthal anisotropy of *Lg* attenuation in eastern Tibetan Plateau. *Journal of Geophysical Research*, *117*(B10), B10309. https://doi.org/10.1029/2012JB009255

Bao, X., Sandvol, E., Zor, E., Sakin, S., Mohamad, R., Gok, R., et al. (2011). Pg attenuation tomography within the northern Middle East. *Bulletin of the Seismological Society of America*, *101*(4), 1496–1506. https://doi.org/10.1785/0120100316

Barazangi, M., Sandvol, E., & Seber, D. (2006). Structure and tectonic evolution of the Anatolian plateau in eastern Turkey. In Y. Dilek & S. Pavlides (Eds.), *Postcollisional tectonics and magmatism in the Mediterranean region and Asia*. Geological Society of America. https://doi.org/10.1130/2006.2409(22)

Bartol, J., & Govers, R. (2014). A single cause for uplift of the Central and Eastern Anatolian plateau? *Tectonophysics*, *637*, 116–136. https://doi.org/10.1016/j.tecto.2014.10.002

Baumont, D., Paul, A., Beck, S., & Zandt, G. (1999). Strong crustal heterogeneity in the Bolivian Altiplano as suggested by attenuation of *Lg* waves. *Journal of Geophysical Research*, *104*(B9), 20287–20305. https://doi.org/10.1029/1999JB900160

Berk Biryol, C., Beck, S. L., Zandt, G., & Özacar, A. A. (2011). Segmented African lithosphere beneath the Anatolian region inferred from teleseismic P-wave tomography: Segmented lithosphere beneath Anatolia. *Geophysical Journal International*, *184*(3), 1037–1057. https://doi.org/10.1111/j.1365-246X.2010.04910.x

Bocchini, G. M., Brüstle, A., Becker, D., Meier, T., van Keken, P. E., Ruscic, M., et al. (2018). Tearing, segmentation, and backstepping of subduction in the Aegean: New insights from seismicity. *Tectonophysics*, *734–735*, 96–118. https://doi.org/10.1016/j.tecto.2018.04.002

Bouchon, M. (1982). The complete synthesis of seismic crustal phases at regional distances. *Journal of Geophysical Research*, *87*(B3), 1735. https://doi.org/10.1029/JB087iB03p01735

Bozkurt, E. (2001). Neotectonics of Turkey – A synthesis. *Geodinamica Acta*, *14*(1–3), 3–30. https://doi.org/10.1080/09853111.2001.11432432

Burke, K. (2011). Plate tectonics, the Wilson cycle, and mantle plumes: Geodynamics from the top. *Annual Review of Earth and Planetary Sciences*, *39*(1), 1–29. https://doi.org/10.1146/annurev-earth-040809-152521

Chen, Y., Gu, Y. J., Mohammed, F., Wang, J., Sacchi, M. D., Wang, R., & Nguyen, B. (2021). Crustal attenuation beneath western North America: Implications for slab subduction, terrane accretion and arc magmatism of the Cascades. *Earth and Planetary Science Letters*, *560*, 116783. https://doi.org/10.1016/j.epsl.2021.116783

Delph, J. R., Abgarmi, B., Ward, K. M., Beck, S. L., Özacar, A. A., Zandt, G., et al. (2017). The effects of subduction termination on the continental lithosphere: Linking volcanism, deformation, surface uplift, and slab tearing in Central Anatolia. *Geosphere*, *13*(6), 1788–1805. https://doi.org/10.1130/GES01478.1

Delph, J. R., Zandt, G., & Beck, S. L. (2015). A new approach to obtaining a 3D shear wave velocity model of the crust and upper mantle: An application to eastern Turkey. *Tectonophysics*, *665*, 92–100. https://doi.org/10.1016/j.tecto.2015.09.031

Faccenna, C., Becker, T. W., Jolivet, L., & Keskin, M. (2013). Mantle convection in the Middle East: Reconciling Afar upwelling, Arabia indentation and Aegean trench rollback. *Earth and Planetary Science Letters*, *375*, 254–269. https://doi.org/10.1016/j.epsl.2013.05.043

Fernández-Blanco, D., Mannu, U., Bertotti, G., & Willett, S. D. (2020). Forearc high uplift by lower crustal flow during growth of the Cyprus-Anatolian margin. *Earth and Planetary Science Letters*, *544*, 116314. https://doi.org/10.1016/j.epsl.2020.116314

Fichtner, A., Saygin, E., Taymaz, T., Cupillard, P., Capdeville, Y., & Trampert, J. (2013). The deep structure of the North Anatolian fault zone. *Earth and Planetary Science Letters*, *373*, 109–117. https://doi.org/10.1016/j.epsl.2013.04.027

Göğüş, O. H., & Pysklywec, R. N. (2008). Mantle lithosphere delamination driving plateau uplift and synconvergent extension in eastern Anatolia. *Geology*, *36*(9), 723. https://doi.org/10.1130/G24982A.1

Göğüş, O. H., Pysklywec, R. N., Şengör, A. M. C., & Gün, E. (2017). Drip tectonics and the enigmatic uplift of the central Anatolian Plateau. *Nature Communications*, *8*(1), 1538. https://doi.org/10.1038/s41467-017-01611-3

Göğüş, O. H., & Ueda, K. (2018). Peeling back the lithosphere: Controlling parameters, surface expressions and the future directions in delamination modeling. *Journal of Geodynamics*, *117*, 21–40. https://doi.org/10.1016/j.jog.2018.03.003

Gök, R., Pasyanos, M. E., & Zor, E. (2007). Lithospheric structure of the continent-continent collision zone: Eastern Turkey. *Geophysical Journal International*, *169*(3), 1079–1088. https://doi.org/10.1111/j.1365-246X.2006.03288.x

Gök, R., Sandvol, E., Türkelli, N., Seber, D., & Barazangi, M. (2003). Sn attenuation in the Anatolian and Iranian plateau and surrounding regions. *Geophysical Research Letters*, *30*(24), 8042. https://doi.org/10.1029/2003GL018020

Granot, R. (2016). Palaeozoic oceanic crust preserved beneath the eastern Mediterranean. *Nature Geoscience*, *9*(9), 701–705. https://doi.org/10.1038/ngeo2784

Hacıoğlu, Ö., Başokur, A. T., & Çiftçi, E. T. (2018). Crustal structure of a young collision zone: The Arabia–Eurasia collision in northeastern Turkey investigated by magnetotelluric data. *Earth Planets and Space*, *70*(1), 161. https://doi.org/10.1186/s40623-018-0932-3

Hayes, G. P., Moore, G. L., Portner, D. E., Hearne, M., Flamme, H., Furtney, M., & Smoczyk, G. M. (2018). Slab2, a comprehensive subduction zone geometry model. *Science*, *362*(6410), 58–61. https://doi.org/10.1126/science.aat4723

He, X., Zhao, L., Xie, X., Tian, X., & Yao, Z. (2021). Weak crust in southeast Tibetan plateau revealed by Lg-Wave attenuation tomography: Implications for crustal material escape. *Journal of Geophysical Research: Solid Earth*, *126*(3), e2020JB020748. https://doi.org/10.1029/2020JB020748

Kaviani, A., Paul, A., Moradi, A., Mai, P. M., Pilia, S., Boschi, L., et al. (2020). Crustal and uppermost mantle shear wave velocity structure beneath the Middle East from surface wave tomography. *Geophysical Journal International*, *221*(2), 1349–1365. https://doi.org/10.1093/gji/ggaa075

Kaviani, A., Sandvol, E., Bao, X., Rümpker, G., & Gök, R. (2015). The structure of the crust in the Turkish–Iranian Plateau and Zagros using Lg Q and velocity. *Geophysical Journal International*, *200*(2), 1254–1268. https://doi.org/10.1093/gji/ggu468

Kaviani, A., Sandvol, E., Ku, W., Beck, S. L., Türkelli, N., Özacar, A. A., & Delph, J. R. (2022). Seismic attenuation tomography of the Sn phase beneath the Turkish-Iranian Plateau and the Zagros mountain belt. *Geosphere*, *18*(4), 1377–1393. https://doi.org/10.1130/GES02503.1

Kennett, B. L. N. (1989). On the nature of regional seismic phases-I. Phase representations for Pn, Pg, Sn, Lg. *Geophysical Journal International*, *98*(3), 447–456. https://doi.org/10.1111/j.1365-246X.1989.tb02281.x

Keskin, M. (2003). Magma generation by slab steepening and breakoff beneath a subduction-accretion complex: An alternative model for collision-related volcanism in Eastern Anatolia, Turkey. *Geophysical Research Letters*, *30*(24), 8046. https://doi.org/10.1029/2003GL018019

Keskin, M. (2007). Eastern Anatolia: A hotspot in a collision zone without a mantle plume. In *Special paper 430: Plates, plumes and planetary processes* (Vol. 430, pp. 693–722). Geological Society of America. https://doi.org/10.1130/2007.2430(32)

Kounoudis, R., Bastow, I. D., Ogden, C. S., Goes, S., Jenkins, J., Grant, B., & Braham, C. (2020). Seismic tomographic imaging of the eastern Mediterranean mantle: Implications for terminal-stage subduction, the uplift of Anatolia, and the development of the North Anatolian Fault. *Geochemistry, Geophysics, Geosystems*, *21*(7), e2020GC009009. https://doi.org/10.1029/2020GC009009

Krischer, L., Megies, T., Barsch, R., Beyreuther, M., Lecocq, T., Caudron, C., & Wassermann, J. (2015). ObsPy: A bridge for seismology into the scientific Python ecosystem. *Computational Science & Discovery*, *8*(1), 014003. https://doi.org/10.1088/1749-4699/8/1/014003

Kürkcüoglu, B., sen, E., Temel, A., Aydar, E., & Gourgaud, A. (2004). Interaction of asthenospheric and lithospheric mantle: The genesis of calc-alkaline volcanism at Erciyes Volcano, Central Anatolia, Turkey. *International Geology Review*, *46*(3), 243–258. https://doi.org/10.2747/0020-6814.46.3.243

Laske, G., Masters, G., Zhitu, M., & Pasyanos, M. E. (2013). Update on CRUST1.0: A 1-degree global model of Earth's crust. Poster No. EGU2013-2658.

Lei, J., & Zhao, D. (2007). Teleseismic evidence for a break-off subducting slab under Eastern Turkey. *Earth and Planetary Science Letters*, *257*(1–2), 14–28. https://doi.org/10.1016/j.epsl.2007.02.011

Le Pichon, X., & Kreemer, C. (2010). The Miocene-to-present kinematic evolution of the eastern Mediterranean and Middle East and its implications for dynamics. *Annual Review of Earth and Planetary Sciences*, *38*(1), 323–351. https://doi.org/10.1146/annurev-earth-040809-152419

Lü, Y., Ni, S., Chen, L., & Chen, Q.-F. (2017). Pn tomography with Moho depth correction from Eastern Europe to western China: *Pn* Tomography from Europe to China. *Journal of Geophysical Research: Solid Earth*, *122*(2), 1284–1301. https://doi.org/10.1002/2016JB013052

Luo, Y., Zhao, L.-F., Ge, Z.-X., Xie, X.-B., & Yao, Z.-X. (2021). Crustal Lg-wave attenuation in Southeast Asia and its implications for regional tectonic evolution. *Geophysical Journal International*, *226*(3), 1873–1884. https://doi.org/10.1093/gji/ggab122

Memiş, C., Göğüş, O. H., Uluocak, E. Ş., Pysklywec, R., Keskin, M., Şengör, A. M. C., & Topuz, G. (2020). Long wavelength progressive plateau uplift in Eastern Anatolia since 20 Ma: Implications for the role of slab peel-back and break-off. *Geochemistry, Geophysics, Geosystems*, *21*(2), e2019GC008726. https://doi.org/10.1029/2019GC008726

Mutlu, A. K., & Karabulut, H. (2011). Anisotropic Pn tomography of Turkey and adjacent regions: Anisotropic Pn tomography of Turkey. *Geophysical Journal International*, *187*(3), 1743–1758. https://doi.org/10.1111/j.1365-246X.2011.05235.x

Nikogosian, I. K., Bracco Gartner, A. J. J., Bergen, M. J., Mason, P. R. D., & Hinsbergen, D. J. J. (2018). Mantle sources of recent Anatolian intraplate magmatism: A regional plume or local tectonic origin? *Tectonics*, *37*(12), 4535–4566. https://doi.org/10.1029/2018TC005219

Paige, C. C., & Saunders, M. A. (1982). LSQR: An algorithm for sparse linear equations and sparse least squares. *ACM Transactions on Mathematical Software*, *8*(1), 43–71. https://doi.org/10.1145/355984.355989

Pasyanos, M. E., Matzel, E. M., Walter, W. R., & Rodgers, A. J. (2009). Broad-band Lg attenuation modelling in the Middle East. *Geophysical Journal International*, *177*(3), 1166–1176. https://doi.org/10.1111/j.1365-246X.2009.04128.x

Pawlewicz, M. J., Steinshouer, D. W., & Gautier, D. L. (1997). *Map showing geology, oil and gas fields, and geologic provinces of Europe including Turkey*. (Open-File Report No. 97- 470I). U.S. Geological Survey.

Portner, D. E., Delph, J. R., Biryol, C. B., Beck, S. L., Zandt, G., Özacar, A. A., et al. (2018). Subduction termination through progressive slab deformation across Eastern Mediterranean subduction zones from updated P-wave tomography beneath Anatolia. *Geosphere*, *14*(3), 907–925. https://doi.org/10.1130/GES01617.1

Rabayrol, F., Hart, C. J. R., & Thorkelson, D. J. (2019). Temporal, spatial and geochemical evolution of late Cenozoic post-subduction magmatism in central and eastern Anatolia, Turkey. *Lithos*, *336–337*, 67–96. https://doi.org/10.1016/j.lithos.2019.03.022

Reid, M. R., Delph, J. R., Cosca, M. A., Schleiffarth, W. K., & Gençalioğlu Kuşcu, G. (2019). Melt equilibration depths as sensors of lithospheric thickness during Eurasia-Arabia collision and the uplift of the Anatolian Plateau. *Geology*, *47*(10), 943–947. https://doi.org/10.1130/G46420.1

Reid, M. R., Schleiffarth, W. K., Cosca, M. A., Delph, J. R., Blichert-Toft, J., & Cooper, K. M. (2017). Shallow melting of MORB-like mantle under hot continental lithosphere, Central Anatolia. *Geochemistry, Geophysics, Geosystems*, *18*(5), 1866–1888. https://doi.org/10.1002/2016GC006772

Reilinger, R., McClusky, S., Vernant, P., Lawrence, S., Ergintav, S., Cakmak, R., et al. (2006). GPS constraints on continental deformation in the Africa-Arabia-Eurasia continental collision zone and implications for the dynamics of plate interactions. *Journal of Geophysical Research*, *111*(B5), B05411. https://doi.org/10.1029/2005JB004051

Rosenberg, C. L., & Handy, M. R. (2005). Experimental deformation of partially melted granite revisited: Implications for the continental crust. *Journal of Metamorphic Geology*, *23*(1), 19–28. https://doi.org/10.1111/j.1525-1314.2005.00555.x

Schildgen, T. F., Yıldırım, C., Cosentino, D., & Strecker, M. R. (2014). Linking slab break-off, Hellenic trench retreat, and uplift of the Central and Eastern Anatolian plateaus. *Earth-Science Reviews*, *128*, 147–168. https://doi.org/10.1016/j.earscirev.2013.11.006

Schleiffarth, W. K., Darin, M. H., Reid, M. R., & Umhoefer, P. J. (2018). Dynamics of episodic late Cretaceous–Cenozoic magmatism across central to eastern Anatolia: New insights from an extensive geochronology compilation. *Geosphere*, *14*(5), 1990–2008. https://doi.org/10.1130/GES01647.1

Şen, P. A., Temel, A., & Gourgaud, A. (2004). Petrogenetic modelling of quaternary post-collisional volcanism: A case study of central and eastern Anatolia. *Geological Magazine*, *141*(1), 81–98. https://doi.org/10.1017/S0016756803008550

Şengör, A. M. C., Özeren, M. S., Keskin, M., Sakınç, M., Özbakır, A. D., & Kayan, İ. (2008). Eastern Turkish high plateau as a small Turkic-type orogen: Implications for post-collisional crust-forming processes in Turkic-type orogens. *Earth-Science Reviews*, *90*(1–2), 1–48. https://doi.org/10.1016/j.earscirev.2008.05.002

Smit, J., Brun, J.-P., Cloetingh, S., & Ben-Avraham, Z. (2010). The rift-like structure and asymmetry of the Dead Sea Fault. *Earth and Planetary Science Letters*, *290*(1–2), 74–82. https://doi.org/10.1016/j.epsl.2009.11.060

Takei, Y. (2017). Effects of partial melting on seismic velocity and attenuation: A new insight from experiments. *Annual Review of Earth and Planetary Sciences*, *45*(1), 447–470. https://doi.org/10.1146/annurev-earth-063016-015820

Toprak, V., Savascin, Y., Gulec, N., & Tankut, A. (1996). Structure of the Galatean volcanic province, Turkey. *International Geology Review*, *38*(8), 747–758. https://doi.org/10.1080/00206819709465358

Türkoğlu, E., Unsworth, M., Çağlar, İ., Tuncer, V., & Avşar, Ü. (2008). Lithospheric structure of the Arabia-Eurasia collision zone in eastern Anatolia: Magnetotelluric evidence for widespread weakening by fluids. *Geology*, *36*(8), 619. https://doi.org/10.1130/G24683A.1

Vanacore, E. A., Taymaz, T., & Saygin, E. (2013). Moho structure of the Anatolian Plate from receiver function analysis. *Geophysical Journal International*, *193*(1), 329–337. https://doi.org/10.1093/gji/ggs107

van Hunen, J., & Miller, M. S. (2015). Collisional processes and links to episodic changes in subduction zones. *Elements*, *11*(2), 119–124. https://doi.org/10.2113/gselements.11.2.119

Varol, E., Temel, A., Yürür, T., Gourgaud, A., & Bellon, H. (2014). Petrogenesis of the Neogene bimodal magmatism of the Galatean volcanic province, Central Anatolia, Turkey. *Journal of Volcanology and Geothermal Research*, *280*, 14–29. https://doi.org/10.1016/j.jvolgeores.2014.04.014

Wang, H., & Currie, C. A. (2015). Magmatic expressions of continental lithosphere removal. *Journal of Geophysical Research: Solid Earth*, *120*(10), 7239–7260. https://doi.org/10.1002/2015JB012112

Wdowinski, S., Ben-Avraham, Z., Arvidsson, R., & Ekström, G. (2006). Seismotectonics of the Cyprian Arc. *Geophysical Journal International*, *164*(1), 176–181. https://doi.org/10.1111/j.1365-246X.2005.02737.x

Wei, Z., Kennett, B. L. N., & Zhao, L.-F. (2017). Lg-wave attenuation in the Australian crust. *Tectonophysics*, *717*, 413–424. https://doi.org/10.1016/j.tecto.2017.08.022

Wessel, P., Luis, J. F., Uieda, L., Scharroo, R., Wobbe, F., Smith, W. H. F., & Tian, D. (2019). The generic mapping tools version 6. *Geochemistry, Geophysics, Geosystems*, *20*(11), 5556–5564. https://doi.org/10.1029/2019GC008515

Zhang, L., Zhao, L.-F., Xie, X.-B., Wu, Q.-J., & Yao, Z.-X. (2022). Lateral variations in crustal Lg attenuation in and around the Hangay Dome, Mongolia. *International Journal of Earth Sciences*, *111*(2), 591–606. https://doi.org/10.1007/s00531-021-02131-8

Zhang, T.-R., & Lay, T. (1995). Why the Lg phase does not traverse oceanic crust. *Bulletin of the Seismological Society of America*, *14*. https://doi.org/10.1785/BSSA0850061665

Zhao, L.-F., & Mousavi, S. M. (2018). Lateral variation of crustal Lg attenuation in eastern North America. *Scientific Reports*, *8*(1), 7285. https://doi.org/10.1038/s41598-018-25649-5

Zhao, L.-F., & Xie, X.-B. (2016). Strong Lg-wave attenuation in the Middle East continental collision orogenic belt. *Tectonophysics*, *674*, 135–146. https://doi.org/10.1016/j.tecto.2016.02.025

Zhao, L.-F., Xie, X.-B., He, J.-K., Tian, X., & Yao, Z.-X. (2013). Crustal flow pattern beneath the Tibetan Plateau constrained by regional Lg-wave Q tomography. *Earth and Planetary Science Letters*, *383*, 113–122. https://doi.org/10.1016/j.epsl.2013.09.038

Zhao, L.-F., Xie, X.-B., Wang, W.-M., Zhang, J.-H., & Yao, Z.-X. (2010). Seismic *Lg*-wave *Q* tomography in and around Northeast China. *Journal of Geophysical Research*, *115*(B8), B08307. https://doi.org/10.1029/2009JB007157

Zhao, L.-F., Xie, X.-B., Wang, W.-M., Zhang, J.-H., & Yao, Z.-X. (2013). Crustal Lg attenuation within the north China Craton and its surrounding regions. *Geophysical Journal International*, *195*(1), 513–531. https://doi.org/10.1093/gji/ggt235

Zhu, H. (2018). High Vp/Vs ratio in the crust and uppermost mantle beneath volcanoes in the Central and Eastern Anatolia. *Geophysical Journal International*, *214*(3), 2151–2163. https://doi.org/10.1093/gji/ggy253

Zor, E., Sandvol, E., Xie, J., Turkelli, N., Mitchell, B., Gasanov, A. H., & Yetirmishli, G. (2007). Crustal attenuation within the Turkish Plateau and surrounding regions. *Bulletin of the Seismological Society of America*, *97*(1B), 151–161. https://doi.org/10.1785/0120050227